

Figure 1. Pseudo-first-order rate constant for the reaction of eq 1, which varies linearly with the concentration of diazomethane in experiments having $[\text{CH}_2\text{N}_2]_0 \gg [\text{X}_2\text{Pt}_2(\mu\text{-dppm})_2]_0$, the latter being varied $(0.5\text{--}14) \times 10^{-5}$ M for $\text{X} = \text{Cl}$. Data are shown for (1) $\text{Pt}_2\text{Cl}_2(\mu\text{-dppm})_2$, (2) $[\text{Pt}_2(\text{Cl})(\text{CO})(\mu\text{-dppm})_2](\text{PF}_6)$, and (3) $[\text{Pt}_2(\text{CO})_2(\mu\text{-dppm})_2](\text{PF}_6)_2$.

Table I. Kinetic Data^a for the Reaction of Dinuclear Pt(I) Complexes with Diazomethane

complex	range of $[\text{CH}_2\text{N}_2]/\text{M}$	$k(2^\circ\text{C})/\text{M}^{-1}\text{s}^{-1}$
$\text{Pt}_2\text{Br}_2(\mu\text{-dppm})_2$	$(0.4\text{--}1) \times 10^{-3}$	204
$\text{Pt}_2\text{I}_2(\mu\text{-dppm})_2$	$(0.2\text{--}1) \times 10^{-3}$	73
$\text{Pt}_2\text{Cl}_2(\mu\text{-dppm})_2$	$(0.5\text{--}2.5) \times 10^{-3}$	41.2 ^b
$\text{Pt}_2(\text{Cl})(\text{CO})(\mu\text{-dppm})_2^+$	$(0.1\text{--}4.5) \times 10^{-3}$	20.6
$\text{Pt}_2(\text{CO})_2(\mu\text{-dppm})_2^{2+}$	$(1\text{--}6) \times 10^{-3}$	1.0
$\text{Pt}_2(\text{C}_6\text{H}_5\text{N})_2(\mu\text{-dppm})_2^{2+}$	1×10^{-3}	$<10^{-2}$
$\text{Pt}_2(\text{NH}_3)_2(\mu\text{-dppm})_2^{2+}$	6×10^{-3}	$<10^{-2}$

^a In CH_2Cl_2 containing up to 2% $(\text{C}_2\text{H}_5)_2\text{O}$ from the diazomethane solutions. Reactions were monitored spectrophotometrically, usually at two or more wavelengths, 240–430 nm. ^b Data as a function of temperature (six values, 2.0–25.0 °C) yield $\Delta H^\ddagger = 14.27 \pm 0.24$ kcal mol⁻¹ and $\Delta S^\ddagger = 0.94 \pm 0.83$ cal mol⁻¹ K⁻¹.

include those bridged by a μ -methylene group, also referred to as “bridging carbene” complexes. In the structural unit $\text{M}-\text{CH}_2-\text{M}$, the two metals are often further joined by a metal–metal bond. The particular μ -methylene complexes that are the subject of this report have no such bond, the product being stabilized against dissociation by the bridging dppm ligands.

The reactions shown, and reactions of the analogous cationic complexes having one or two neutral ligands in place of halide,⁶ were studied in purified dichloromethane. UV–visible spectrophotometry and product isolation showed that they proceed cleanly as written, with no detectable concentration of any reaction intermediate building up during the course of the reaction.^{7,8} Kinetic data were obtained in experiments employing a large excess of diazomethane (Figure 1). Over wide concentration ranges a second-order rate law (eq 2) applies,

$$\frac{d[\text{X}_2\text{Pt}_2(\mu\text{-dppm})_2(\mu\text{-CH}_2)]}{dt} = k[\text{X}_2\text{Pt}_2(\mu\text{-dppm})_2][\text{CH}_2\text{N}_2] \quad (2)$$

leading to the rate constants summarized in Table I. The reactions were unaffected by oxygen or moisture.

The significant features of these results are as follows: (1) The rate drops off sharply when both halides are replaced by neutral amine and pyridine ligands, and even the carbonyl complex reacts only 2% as rapidly as the slowest of the halides. (2) Relatively smaller (and irregular) rate variations are found among the dihalides, Cl (41) $<$ Br (204) $>$ I ($73 \text{ M}^{-1} \text{ s}^{-1}$). (3) The rate constants are characterized by an activation entropy which is nearly zero. These points argue against a mechanism in which the rate-limiting step is attack of the methylene group of $\text{N}\equiv\text{N}^+-\text{CH}_2$ on the electropositive metal center: Such a mechanism would be facilitated by replacement of the negative halide by a neutral ligand and, being a bimolecular, bond-making process, would be characterized by a substantial, negative value of ΔS^\ddagger .

Rather, the data suggest rate-limiting transfer of an electron pair from the metal–metal bond to the methylene group of diazomethane. Both effects described are in accord with this formulation. The value of $\Delta S^\ddagger \approx 0$ is the result of offsetting contributions from organizational terms and from the weakening of the N–C bond preceding the liberation of N_2 . The clear implication is that diazomethane acts as an electrophile toward the metal–metal bond. To our knowledge, this is the first such demonstration. Initial coordination to platinum through nitrogen seems unlikely in that it would appear not to facilitate the overall chemical change represented by eq 1. Further work on related reactions is in progress.

Acknowledgment. This work was supported by the Chemical Sciences Division of the Office of Basic Energy Sciences of the U.S. Department of Energy under contract W-7405-ENG-82.

Ames Laboratory and the Department of Chemistry
Iowa State University
Ames, Iowa 50011

S. Muralidharan
James H. Espenson*

Received May 24, 1983

Characterization of a Unique Electrochemical Oxidation Catalyst: The Difluoro Complex of Iron(III) Tetraphenylporphyrin

Sir:

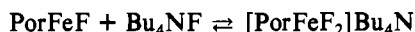
It has been known for some time that two fluoride ions will bind to iron(III) porphyrins in aprotic solvents to form six-coordinate high-spin complexes.^{1–3} More recently it has been reported that reductive electrochemistry of $(\text{TPP})\text{FeF}_2^-$ is distinctive in that the two fluoride ions shift the iron(III) \rightarrow iron(II) couple to -1.10 V (all potentials are referenced to the saturated calomel electrode).^{3,4} By comparison the couple for the monofluoro complex is -0.50 V.³ We have found that the oxidation of $(\text{TPP})\text{FeF}_2^-$ is also unique, as the first ox-

- (6) Brown, M. P.; Franklin, S. J.; Puddephatt, R. J.; Thomson, M. A.; Seddon, K. R. *J. Organomet. Chem.* **1979**, *178*, 281. The cationic complexes were prepared and used as their hexafluorophosphate salts.
- (7) The UV–visible spectra of these complexes, which do not appear to have been reported previously, are quite characteristic. Complete details will be published in the full paper, but the following is typical: $\text{Cl}_2\text{Pt}_2(\mu\text{-dppm})_2(\mu\text{-CH}_2)$ λ_{max} 376 (ϵ $5.2 \times 10^3 \text{ M}^{-1} \text{ cm}^{-1}$), 308 (shoulder) (7.5×10^3), and 264 nm (2.6×10^4). The product solutions from kinetic determinations have absorption spectra that agree precisely with those of the authentic crystalline μ -methylene complexes in every instance. The rate constants were, in every case, independent of the monitoring wavelength.
- (8) Cationic $\mu\text{-CH}_2$ complexes of this family do not appear to have been prepared and characterized previously. The compound $[\text{Pt}_2(\text{PPh}_3)_2(\mu\text{-CH}_2)(\mu\text{-dppm})_2](\text{PF}_6)_2$ has λ_{max} 372 cm (ϵ $5.7 \times 10^3 \text{ M}^{-1} \text{ cm}^{-1}$). ¹H NMR (CD_2Cl_2 with Me_4Si reference): $\mu\text{-CH}_2$ (2 H), δ 1.2, multiplet; CH_2 of dppm (4 H), δ 3.6 and 5.05, multiplets (i.e., the latter CH_2 groups are inequivalent in the A-frame product as compared to the case in the starting complex). ³¹P NMR (¹H decoupled, CD_2Cl_2 with H_3PO_4 reference): $(\text{Ph}_2\text{P})_2\text{CH}_2$, δ 20.8; Ph_2P , δ 32.76.

- (1) Momenteau, M.; Mispelter, J.; Lexa, D. *Biochim. Biophys. Acta* **1973**, *320*, 652.
- (2) Gans, P.; Marchon, J. C.; Moulis, J. M. *Polyhedron* **1982**, *1*, 737.
- (3) Bottomley, L. A.; Kadish, K. M. *Inorg. Chem.* **1981**, *20*, 1348.
- (4) Porphyrin abbreviations: TPP, *meso*-tetraphenylporphyrin; TPP(*p*-OCH₃), *meso*-tetrakis(*p*-methoxyphenyl)porphyrin; OEP, octaethylporphyrin. Abbreviations for salts: $\text{Bu}_4\text{NF}\cdot 3\text{H}_2\text{O}$, tetrabutylammonium fluoride trihydrate; Bu_4NClO_4 , tetrabutylammonium perchlorate.

duction wave is at +0.68 V. This potential is considerably less anodic than that of a large number of five-coordinate high-spin iron(III) tetraphenylporphyrin complexes for which the first oxidation potential is approximately 1.1 V.^{3,5} Fluoride coordination is generally associated with stabilization of elevated oxidation states, and in a thermodynamic sense this accounts for the cathodic shift of the difluoro complex. However, kinetic stability of the oxidized difluoro complex is surprisingly low. Accordingly, we have been unable to isolate the oxidized species but have exploited the novel redox chemistry of (TPP)FeF₂⁻ for catalytic electrochemical oxidations of olefin compounds.

The monofluoro iron(III) TPP, TPP(*p*-OCH₃), and OEP were prepared^{2,6} by shaking the appropriate μ -oxo dimeric species dissolved in methylene chloride with 1 M aqueous HF. The solid product was obtained by slow addition of heptane to the methylene chloride solution. Addition of the trihydrated fluoride salt Bu₄NF·3H₂O (Alfa) to monofluoro iron(III) porphyrin solutions (methylene chloride solvent) is associated with striking changes in the visible region spectra. Spectral changes were equivalent to those noted previously for dimethyl sulfoxide solutions.³ Binding constants for the equilibrium



were determined by the method of Rose and Drago.⁷ For the (TPP)FeF complex the equilibrium quotient is $4.0 \times 10^3 \text{ M}^{-1}$ at 25 °C. Addition of the fluoride salt to (OEP)FeF solution did not yield well-defined isosbestic points, and the presence of more than two species is indicated. The affinity of the second fluoride ion appears to be somewhat lower in the case of (OEP)FeF. In chloroform solution binding constants were approximately 3 orders of magnitude lower as compared with those in methylene chloride. This dramatic effect is presumably due to hydrogen bonding of fluoride with CHCl₃.

Proton NMR spectra at 360 MHz revealed pyrrole signals at 80 and 85 ppm for (TPP)FeF and (TPP)FeF₂⁻, respectively (CD₂Cl₂ solvent, 25 °C). The para phenyl proton signal is at 7.0 ppm for (TPP)FeF and at 8.1 ppm for (TPP)FeF₂⁻. The out-of-plane iron atom in (TPP)FeF induces splitting of meta and ortho phenyl proton signals, giving a meta phenyl doublet at 11.6/10.8 ppm and one resolved component of the presumed ortho phenyl doublet at 8.5 ppm. These signals are collapsed to respective singlets at 8.6 and 10.1 ppm for the (TPP)FeF₂⁻ complex. No splitting was observed at temperatures as low as -64 °C, indicating that rapid ligand exchange was not the cause of doublet collapse. One can reasonably conclude that trans fluoride coordination (rather than cis coordination) places the iron atom effectively in the porphyrin plane to yield a plane of symmetry in the macrocycle. The hyperfine chemical shift values observed for (TPP)FeF₂⁻ are entirely consistent with a high-spin iron(III) configuration, although the pyrrole proton value at 85 ppm is unusual when compared with those of five-coordinate complexes (pyrrole at 79 ppm) and the six-coordinate bis(dimethyl sulfoxide) complex (pyrrole at 64 ppm).^{8,9}

The solution-phase magnetic moment was determined by the method of Evans¹⁰ for (TPP)FeF₂⁻ generated in situ in methylene chloride. The value of $6.0 \pm 0.2 \mu_B$ matches the

Scan Rate, mV/sec

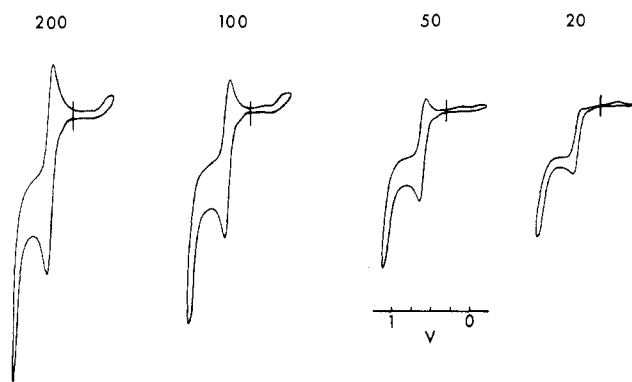


Figure 1. Variable scan rate cyclic voltammetric waves for (TPP)FeF₂⁻ (1 mM) in CH₂Cl₂, containing 0.10 M Bu₄NClO₄ and 0.004 M Bu₄NF·3H₂O, 25 °C. Potentials are referenced to the SCE by using a Ag/0.10 M AgNO₃/acetonitrile secondary reference electrode.

spin-only moment for high-spin iron(III). The EPR spectra of the difluoro complexes were also typical for high-spin iron(III) porphyrins with strong signals at $g = 5.9$ and weak $g = 2$ signals. It was recently reported that no hyperfine structure was apparent for the $g = 2$ signal of (TPP)FeF₂⁻ in methylene chloride at 80 K.² A triplet $g = 2$ signal is expected due to interaction of the two fluorides and this pattern has been observed for difluorodeuterohemin IX dimethyl ester.¹ However, in deoxygenated 1:1 methylene chloride/toluene, which forms better glasses than methylene chloride, and at concentrations of $5 \times 10^{-4} \text{ M}$, we have observed a triplet structure with a coupling constant of 35 G. The same coupling constant is observed for the (OEP)FeF₂⁻ and (TPP(*p*-OCH₃))FeF₂⁻ complexes, but linewidths are quite different. Hyperfine interactions show up only as shoulders for (TPP)FeF₂⁻ and (OEP)FeF₂⁻, but in the case of (TPP(*p*-OCH₃))FeF₂⁻ the splitting is completely resolved.

Cyclic voltammetry of (TPP)FeF₂⁻ revealed a quasi-reversible oxidation wave at 0.68 V, as can be seen in Figure 1.¹¹ Decreasing the scan rate results in a decrease in the ratio of the height of the reduction wave to the height of the oxidation wave. This is in contrast to the (TPP)FeCl complex for which the ratio is constant. The implication is that the oxidized species is not long-lived. Attempts to prepare and isolate the oxidized difluoro complex were unsuccessful. The oxidized monofluoro complex was successfully isolated by procedures previously employed for the chloro analogue.¹³ Addition of the fluoride salt to a methylene chloride solution of the oxidized monofluoro complex at -50 °C gave an obvious and immediate color change to that of the unoxidized difluoro complex. A proton NMR spectrum at -50 °C confirmed that the product of the reaction was (TPP)FeF₂⁻.

The first oxidation wave for other five-coordinate high-spin iron(III) tetraphenylporphyrin adducts is $1.10 \pm 0.05 \text{ V}$.^{5,12}

- (5) Phillippi, M. A.; Shimomura, E. T.; Goff, H. M. *Inorg. Chem.* **1981**, *20*, 1322.
- (6) Cohen, I. A.; Summerville, D. A.; Ru, S. R. *J. Am. Chem. Soc.* **1976**, *98*, 5813.
- (7) Drago, R. S., "Physical Methods in Chemistry"; Saunders: Philadelphia, PA, 1977; pp 88-92.
- (8) La Mar, G. N.; Walker, F. A. In "The Porphyrins"; Dolphin, D., Ed.; Academic Press: New York, 1978; Vol. IV, pp 61-157.
- (9) Goff, H. M. In "Iron Porphyrins—Part I"; Lever, A. B. P., Gray, H. B., Eds.; Addison-Wesley: Reading, MA, 1982; pp 237-281.
- (10) Evans, D. F. *J. Chem. Soc.* **1959**, 2003.

- (11) A Ag/0.10 M AgNO₃/acetonitrile reference electrode separated from the bulk solution by porous Vycor was employed. Ferrocene oxidation was monitored to demonstrate reversibility of the cell configuration. Potentials were adjusted to the conventional aqueous SCE reference¹² by using a factor of 0.38 V. This correction factor was determined by comparing apparent potentials for iron porphyrins (1 mM) dissolved in CH₂Cl₂ (0.1 M Bu₄NClO₄), employing in separate experiments the PAR aqueous SCE electrode and the PAR Ag/0.10 M AgNO₃/acetonitrile electrode. Significant junction potentials are ignored in referencing the aqueous SCE electrode for apolar organic solvents.¹² For purposes of using ferrocene to correct junction potentials, it should be noted that the first oxidation potential of (TPP)FeF₂⁻ is 0.16 V anodic of ferrocene oxidation.
- (12) Kadish, K. M. In "Iron Porphyrins—Part II"; Lever, A. B. P., Gray, H. B., Eds.; Addison-Wesley: Reading, MA, 1983; pp 161-249.
- (13) Phillippi, M. A.; Goff, H. M. *J. Am. Chem. Soc.* **1982**, *104*, 6026.

It is well established that this potential is associated with porphyrin-centered oxidation and π -cation-radical formation.¹³ The lower oxidation potential of $(\text{TPP})\text{FeF}_2^-$ and the high reactivity of the oxidized product suggest an electronic structure different from that of oxidized five-coordinate complexes. Metal-centered oxidation of $(\text{TPP})\text{FeF}_2^-$ to give an iron(IV) species is a viable possibility. The short lifetime of this species could be explained by subsequent oxidation of solvent and/or supporting electrolyte mediated by trace amounts of water.

The high reactivity of oxidized $(\text{TPP})\text{FeF}_2^-$ suggested that the transient, electrochemically generated species could be utilized to effect the functionalization of organic substrates. Accordingly, methylene chloride solutions containing 10% cyclohexene, $(\text{TPP})\text{FeF}_2^-$ (1 mM, generated from $(\text{TPP})\text{FeF}$ and excess $\text{Bu}_4\text{NF}\cdot 3\text{H}_2\text{O}$), and Bu_4NClO_4 (0.1 M) were electrolyzed at potentials slightly anodic of the observed oxidation wave by using a platinum basket working electrode.¹⁴ Volatile components were then separated from supporting electrolyte, excess fluoride salt, and iron porphyrin by flash vacuum distillation. The volatile mixture was analyzed by gas chromatography and gas chromatography-mass spectrometry. The principal oxidation products were found to be cyclohexenone, 2-cyclohexenol, and cyclohexene oxide. No oxidized hydrocarbons were detected if either the monofluoro iron(III) porphyrin or the fluoride salt was excluded from the solution. The small quantity of water introduced from the hydrated salt apparently provides a source of oxygen. Experiments designed to optimize yields, control product ratios, and discern mechanisms are in progress.

Acknowledgment. Support from National Science Foundation Grant CHE 82-09308 is gratefully acknowledged. The Bruker WM-360 NMR spectrometer was purchased in part with National Science Foundation Grant CHE 82-01836.

Registry No. $(\text{TPP})\text{FeF}$, 55428-47-2; $(\text{TPP})\text{FeF}_2^-$, 76402-68-1; $(\text{OEP})\text{FeF}_2^-$, 86668-09-9; $(\text{TPP}(p\text{-OMe}))\text{FeF}_2^-$, 86646-34-6; Bu_4NF , 429-41-4; cyclohexene, 110-83-8.

(14) Addition of cyclohexene had no apparent effect on the variable-rate cyclic voltammetry profiles. This is likely due to the fact that cyclohexene (at the 10% level) is relatively no more reactive toward the oxidized iron porphyrin species than the solvent and/or supporting electrolyte.

Department of Chemistry
University of Iowa
Iowa City, Iowa 52242

David L. Hickman
Harold M. Goff*

Received May 26, 1983

Interstitial and Intercalation Chemistry of the Double-Metal-Layered Yttrium Monochloride

Sir:

The particular monohalides ZrCl ,¹ ZrBr ,² ScCl ,³ and YCl ⁴ as well as those of many lanthanide elements⁵ all provide a novel metal-like array within tightly bound slabs composed of four cubic-close-packed layers sequenced X-M-M-X. Two (Sc, Y etc.) or three (Zr) electrons per metal provide strong bonding of the double-metal layers, and the compounds appear to be metallic. We report that an extensive chemistry exists

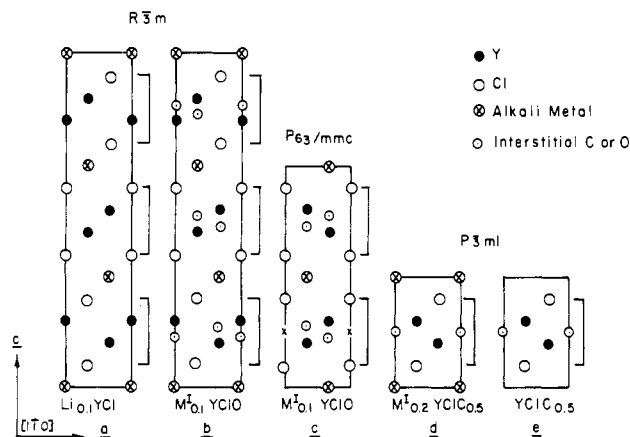


Figure 1. The (110) sections of (a) $3R\text{-Li}_{0.09}\text{YCl}$, (b) $3R\text{-M}_{1.01}^1\text{YClO}$, (c) $2H\text{-M}_{1.01}^1\text{YClO}$, (d) $1T\text{-M}_{1.02}^1\text{YClC}_{0.5}$, and (e) $1T\text{-YClC}_{0.5}$. (The small \times in part c marks the correct origin.)

for YCl and presumably for other related phases; this involves compounds in which there has been interstitial insertion of small non-metals within the tetrahedral or trigonal-antiprismatic (TAP) interstices between the double-metal layers as well as simultaneous or separate intercalation of alkali-metal cations in the van der Waals gap between the chlorine layers with concomitant reduction of the metal layers. Compounds of the latter type are well-known for layered chalcogenides and other phases⁶ but not heretofore for binary halides.⁷ The insertion of hydrogen or oxygen in the tetrahedral metal interstices in ZrCl and ZrBr is already known, giving either $\text{ZrXH}_{0.5}$ and ZrXH where the four-layer slabs are restructured but retained⁸ or ZrXO_y , with continuous variation of the amount of oxygen up to $y \sim 0.4$.⁹ On the other hand, the synthesis of intercalation compounds of the ZrX phases has to date not succeeded.^{2,9}

The new phases $\text{Li}_{0.09}\text{YCl}$, $\text{ScClC}_{0.5}$, $\text{YClC}_{0.5}$, $\text{M}_{1.01}^1\text{YClO}$ (two types), and $\text{M}_{1.02}^1\text{YClC}_{0.5}$ ($M = \text{Li-Cs}$) are all synthesized as black plates by stoichiometric reaction of metal powder or strips with the trichloride and, as appropriate, M^1Cl , Y_2O_3 , YOCl , or C within sealed tantalum tubing at 950°C for 1-3 weeks. The yields for all but $\text{Li}_{0.09}\text{YCl}$ are above 90%. The products are necessarily thermodynamically stable at high temperatures and well crystallized, in contrast to many reported intercalation compounds. The structures of six phases have been solved by single-crystal methods: $\text{Li}_{0.09}\text{YCl}$ ($3R^{10}$), $\text{Na}_{0.08}\text{YClO}_{1.0}$ ($3R$), $\text{K}_{0.08}\text{YClO}_{0.8}$ ($2H$), $\text{ScClC}_{0.56}$ ($1T$), $\text{K}_{0.26}\text{YClC}_{0.4}$ ($1T$), and the parent YCl ($3R$). The alkali-metal, oxygen, and carbon coefficients are the refined values (neutral atoms). Those for oxygen and carbon do not differ significantly from full occupancy, 1.0 and 0.5, respectively, which will be assumed for brevity. The alkali-metal coefficients (x), which have in several cases been verified by microprobe analysis, would be 0.5 for full occupancy in all structures. Other phases isostructural with these have been identified with the aid of high-resolution (Guinier) X-ray powder diffraction and lattice constants refined therefrom by least-squares methods.

The crystal structures of the five new classes of compounds are shown schematically in Figure 1 as conventional (110)

- (1) Adolphson, D. G.; Corbett, J. D. *Inorg. Chem.* **1976**, *15*, 1820.
- (2) Daake, R. L.; Corbett, J. D. *Inorg. Chem.* **1977**, *16*, 2029.
- (3) Poeppelmeier, K. R.; Corbett, J. D. *Inorg. Chem.* **1977**, *16*, 294.
- (4) Mattausch, H.; Hendricks, J. B.; Eger, R.; Corbett, J. D.; Simon, A. *Inorg. Chem.* **1980**, *19*, 2128.
- (5) Mattausch, H.; Simon, A.; Holzer, N.; Eger, R. *Z. Anorg. Allg. Chem.* **1980**, *466*, 7.

- (6) Whittingham, M. S.; Jacobson, A. J., Eds. "Intercalation Chemistry"; Academic Press: New York, 1982.
- (7) Some oxyhalides with the FeOCl structure have been intercalated by alkali metals generally by low-temperature routes; see: Halbert, T. R. Reference 6, Chapter 12.
- (8) Marek, H. S.; Corbett, J. D.; Daake, R. L. *J. Less-Common Met.* **1983**, *89*, 243.
- (9) Seaverson, L. M.; Corbett, J. D. *Inorg. Chem.*, in press.
- (10) This prefix indicates the number of slabs perpendicular to the c axis in the cell repeat and, by R, H or T, whether the symmetry is rhombohedral, hexagonal, or trigonal.